Progress In Electromagnetics Research M, Vol. 85, 185–194, 2019

Artificial Dielectric Superstrate Loaded Antenna for Enhanced Radiation Performance

Devassy Tony[1], Valiyaveettil P. Sarin[2], Neeraj K. Pushkaran[1], Kokkadan J. Nelson[1], Pezholil Mohanan[1], and Kesavath Vasudevan[1, *]

Abstract—This paper presents a novel engineered artificial dielectric superstrate for improving the radiation characteristics of a CPW-fed planar antenna. Even though the permittivity of the material used for the superstrate is only 4.4, it attains an effective permittivity of more than 18 because of the periodic pattern printed on it. Due to the high value of effective permittivity, an improvement in radiation pattern, impedance matching, and gain of the antenna are obtained. From the measured results, an impedance bandwidth of 374 MHz from 2.453 GHz to 2.827 GHz is observed for the antenna loaded with superstrate. The periodic pattern is fabricated on a substrate of thickness 1.6 mm, and it occupies an area of $56.45 \times 42.48\,\text{mm}^2$.

1. INTRODUCTION

The performance of printed circuit antennas used for outdoor applications were affected by environmental hazards, severe weather conditions, etc. A superstrate layer, also called a cover layer has been used to protect the antenna from these threats. Initially, it was assumed that when we used a cover layer, it would adversely affect the matching and radiation performance of the antenna. Alexopoulos and Jackson showed that by a proper selection of superstrate layer, it was possible to enhance the radiation parameters of printed antennas [1]. In [2], transmission line analogy was used to explain radiation from superstrate loaded antenna structure. There the authors established two dual resonance conditions for substrate-superstrate printed antenna geometry by which better gain could be achieved for a high value of permittivity or permeability of the superstrate. In [3], the authors performed a comparative study of three superstrates, namely double negative slab, frequency selective surface, and plain dielectric slab for improving directivity of microstrip antennas. The authors came to the conclusion that the physical mechanism behind directivity enhancement was not the focussing effect of superstrate alone. They attributed the directivity enhancement to the resonance resulting from Fabry-Perot resonant cavity formed by the superstrate and metallic ground plane. Researchers started showing greater interest in developing new methods by which antenna parameters can be improved by manipulating material parameters of superstrates as well as by other means [4–13, 16]. They successfully implemented superstrates in beam steering, enhancing gain, and improving bandwidth. Some authors proposed EBG structures as superstrates for improving antenna parameters [4, 5, 17]. But the thickness of the antenna was the main barrier for these structures. Kim et al. proposed a holey dielectric superstrate for enhancing the gain of a microstrip patch antenna [8]. The effective permittivity was controlled by changing the radius of holes in the superstrate so as to generate an in-phase electric field which resulted in improved gain.

In this paper, a technique for improving the radiation parameters of a CPW-fed planar antenna using a non-resonant superstrate is proposed. It is based on a novel engineered artificial dielectric with

Received 28 June 2019, Accepted 24 September 2019, Scheduled 5 October 2019

* Corresponding author: Kesavath Vasudevan (vasudevankdr@gmail.com).

[1] Department of Electronics, Cochin University of Science and Technology, Cochin-22, Kerala, India. [2] Government College, Chittur, Palakkad, Kerala, India.

high value of effective permittivity. When we load an antenna with a superstrate layer having a high value of permittivity or permeability, the gain can be enhanced [1, 2]. Simulated and experimental results are presented. The effect of artificial dielectric on antenna reflection characteristics, gain, and radiation pattern are investigated.

2. PERIODIC PATTERN DESIGN

For the construction of artificial dielectric, a periodic pattern is used. The pattern consists of 3×4 array of unit cells. The geometry of the unit cell is formed in the following manner. Consider two cylinders of same radius 2 mm and another one of radius 6 mm. All the cylinders are of negligible thickness and made up of highly conductive material. They are placed at the centre of an FR-4 substrate of size $14 \times 14 \times 1.6\,\text{mm}^3$ and relative permittivity 4.4. The thickness of the metallization etched on the substrate is 35 µm. The two cylinders of radius 2 mm are shifted by 4.2 mm in opposite directions along a straight line which makes an angle 45° with Y axis (Fig. 1).

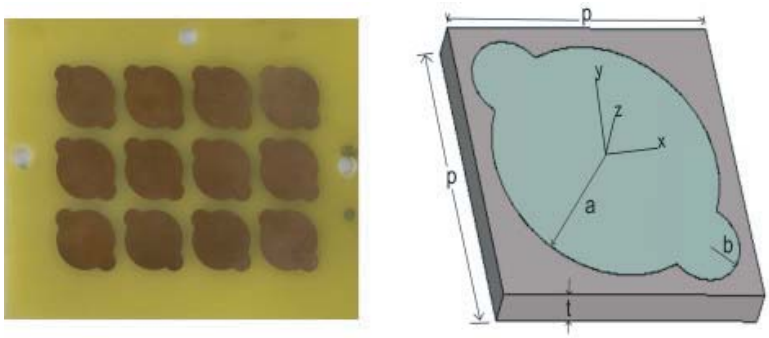

Figure 1. Photograph of the superstrate and unit cell description. $p = 14$, $a = 6$ and $b = 2$ (units in mm).

The array pattern is printed on an FR-4 substrate with relative permittivity 4.4, thickness 1.6 mm, and occupies an area of $56.45 \times 42.48\,\text{mm}^2$. For computing scattering parameters (S parameters) of the periodic pattern by simulation, CST Microwave Studio is used. Along X and Y directions unit cell boundary conditions are applied. These are combined with open boundaries along Z directions. The open boundaries are realized by Floquet mode waveguide ports which can be used for exciting plane waves (Fig. 2).

For characterising artificially engineered materials retrieval of effective permittivity and effective permeability is required. The usual method is to use S parameters calculated from the incident wave

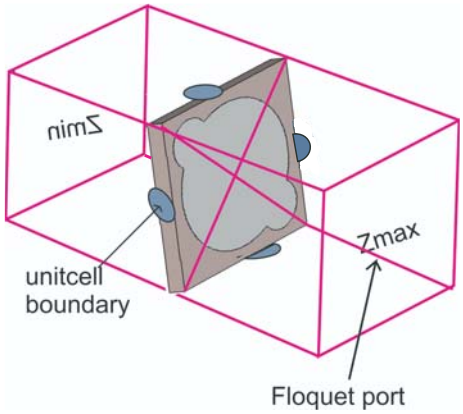

Figure 2. Assignment of Floquet ports and unit cell boundary.

to obtain effective refractive index n and impedance z. The effective permittivity and permeability can then be calculated directly from the expressions $\mu = nz$ and $\epsilon = n/z$.

The refractive index n and impedance z of a slab of material can be obtained from the following expressions [14, 15],

$$z = \pm\sqrt{\frac{(1+S_{11})^2 - S_{21}^2}{(1-S_{11})^2 - S_{21}^2}} \tag{1}$$

$$e^{ink_0d} = X \pm i\sqrt{1-X^2} \tag{2}$$

where $X = 1/2S_{21}(1 - S_{11}^2 + S_{21}^2)$. k_0 denotes the wave number of the incident wave in free space, and d is the thickness of the slab. For a passive medium, the signs of the above equations are determined by the requirement

$$z' \geq 0 \tag{3}$$

$$n'' \geq 0 \tag{4}$$

where $(.)'$ and $(.)''$ denote the real part and imaginary part operators, respectively. Since Equation (2) is a complex exponential, inverting it will result in a multivalued logarithmic function. Solving for refractive index we get

$$n = \frac{1}{k_0 d}\left\{\left[\left[\ln\left(e^{ink_0d}\right)\right]'' + 2m\pi\right] - i\left[\ln\left(e^{ink_0d}\right)\right]'\right\} \tag{5}$$

where m is the branch number of n'.

When we use the above equations for a nonhomogeneous slab, some issues need to be addressed. We have to determine the location of the two boundaries of the effective slab. The retrieval method will fail if the S parameters obtained are noisy. Another issue is ambiguous nature of n' because the logarithmic function is multivalued. All these issues are addressed in [14].

The magnitudes of reflection and transmission characteristics are illustrated in Fig. 3. No resonances are observed in the frequency range shown in figure. Extracted values of effective permittivity and effective permeability are shown in Fig. 4. In [15], the medium is described as having effective permittivity independent of frequency whereas the effective permeability is a function of frequency. From Fig. 4 it is clear that the same pattern can also be observed here, though the magnetic response of the superstrate medium is very feeble. The effective permittivity of the superstrate medium is a function of inter-cell capacitance.

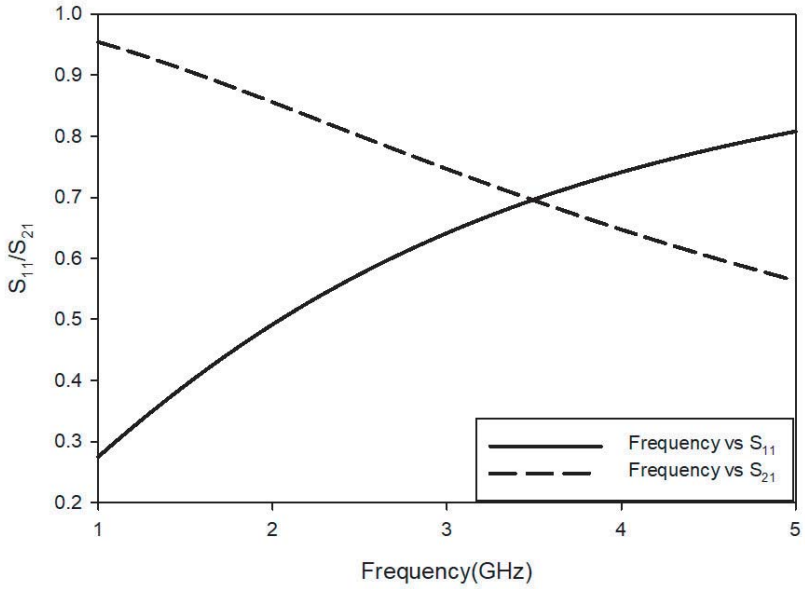

Figure 3. Reflection and transmission characteristics of the unit cell.

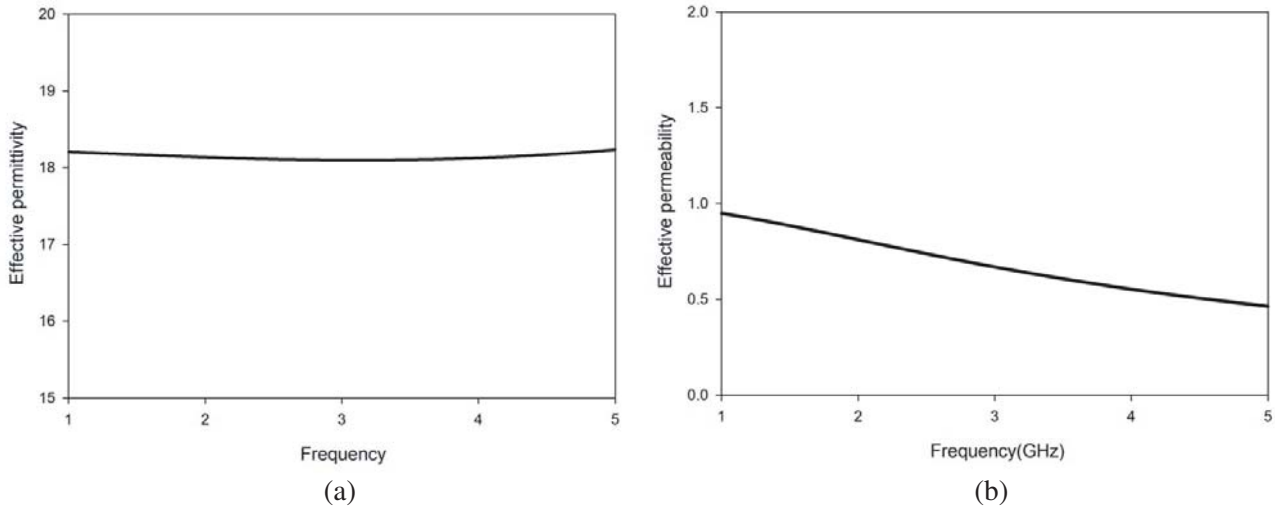

Figure 4. Extracted values of (a) effective permittivity and (b) effective permeability.

3. THE REFERENCE ANTENNA DESIGN

The reference antenna shown in Fig. 5 can be obtained from a standard CPW transmission line by applying a few modifications. First, a 50 Ω CPW transmission line is designed. Standard design equations are used to determine centre conductor width (Wf) and the gap (g) between finite ground planes and centre conductor [18]. The two finite ground planes ($g1$ and $g2$) on either side of the centre conductor are of equal size ($Wg \times Lg$). For a wide range of frequencies extending up to several GHz, there is no resonance observed for this transmission line. The ground $g1$ is connected to the centre conductor using a short of width t to generate a resonance around 3.4 GHz. The resonance can be brought to a lower frequency region by carving out a slot of length Ls in ground $g1$. The reference antenna is printed on an FR-4 substrate with a dielectric constant of 4.4. Overall size of the substrate is $45 \times 21 \times 1.6\,\text{mm}^3$.

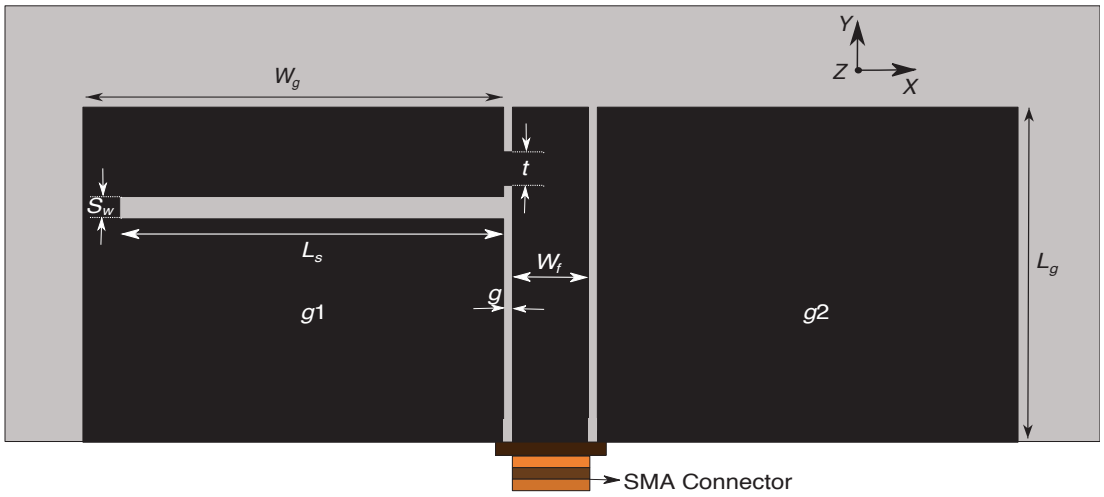

Figure 5. Top view of the reference antenna. $L_s = 13.15$, $L_g = 15$, $S_w = 1$, $W_f = 3$, $W_g = 16.6$, $g = 0.35$ and $t = 1.5$ (units in mm).

4. RESULTS AND DISCUSSIONS

4.1. Reference Antenna

The simulated and measured reflection characteristics of the antenna is shown in Fig. 6. From the measured results, an impedance bandwidth of 325 MHz from 2.5 GHz to 2.825 GHz is observed. The co- and cross-polar radiation patterns of the reference antenna for XZ and YZ planes at 2.62 GHz are shown in Fig. 7. Cross-polar isolation of more than 10 dB along boresight is observed in both planes.

The surface current distribution of the reference antenna at resonance is shown in Fig. 8. The

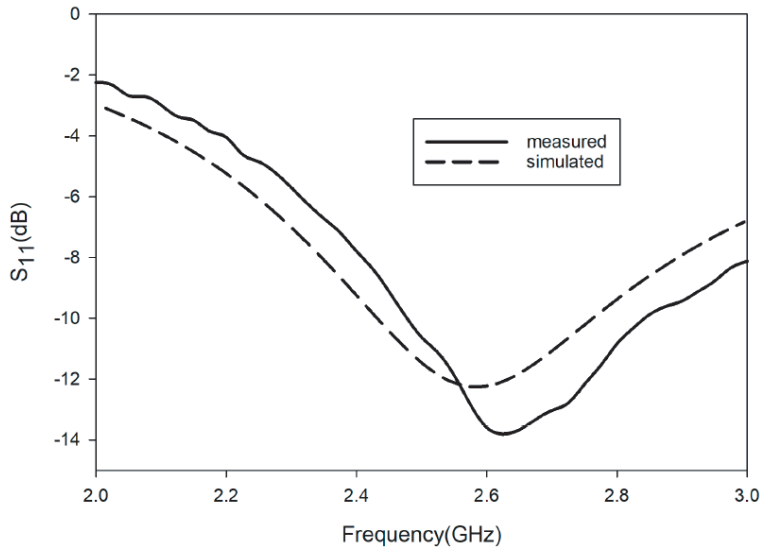

Figure 6. Measured and simulated reflection characteristics.

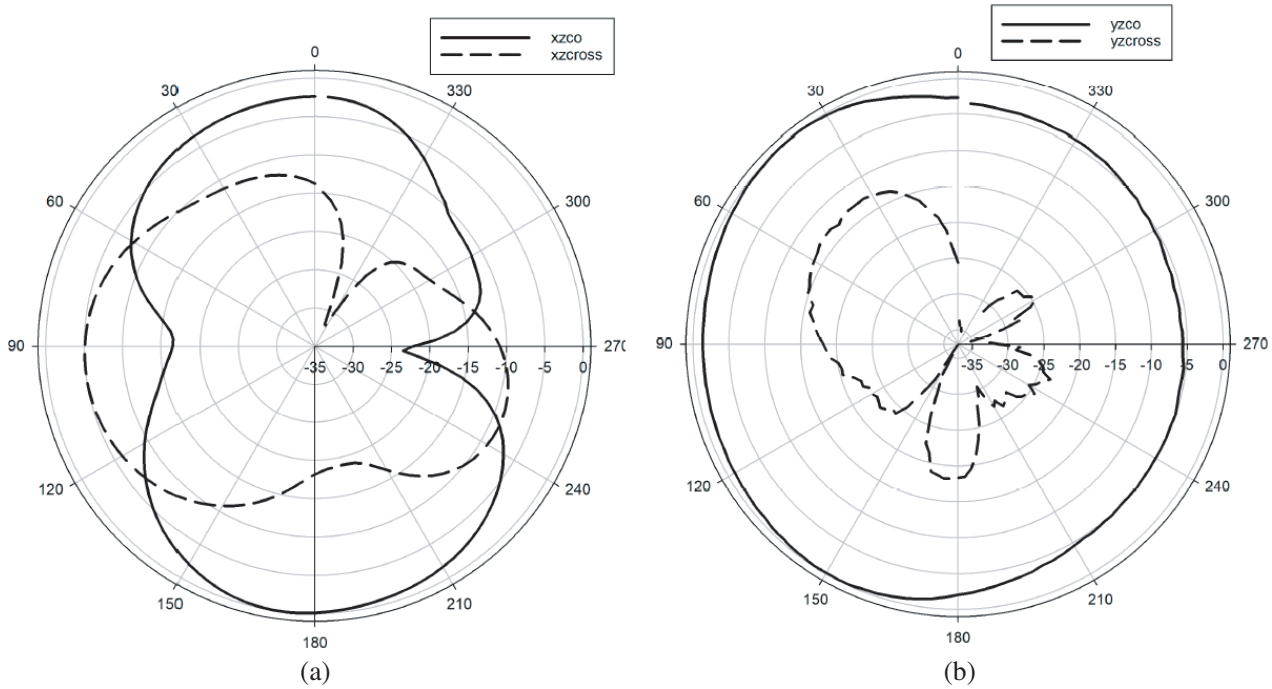

Figure 7. Co and cross polar radiation pattern. (a) XZ plane. (b) YZ plane.

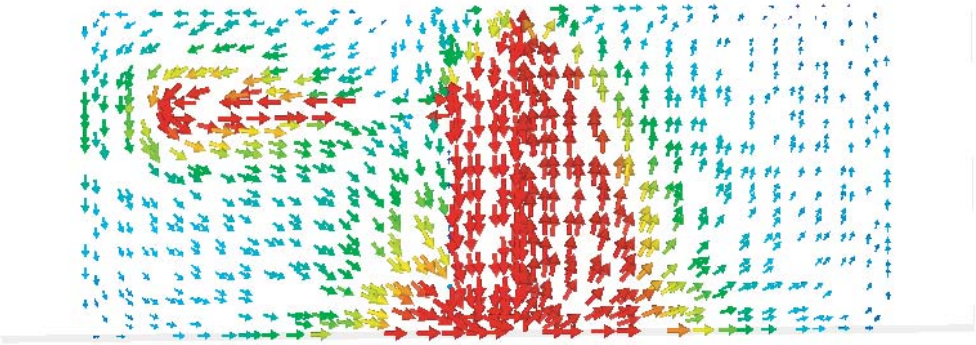

Figure 8. Surface current distribution of the reference antenna at resonance.

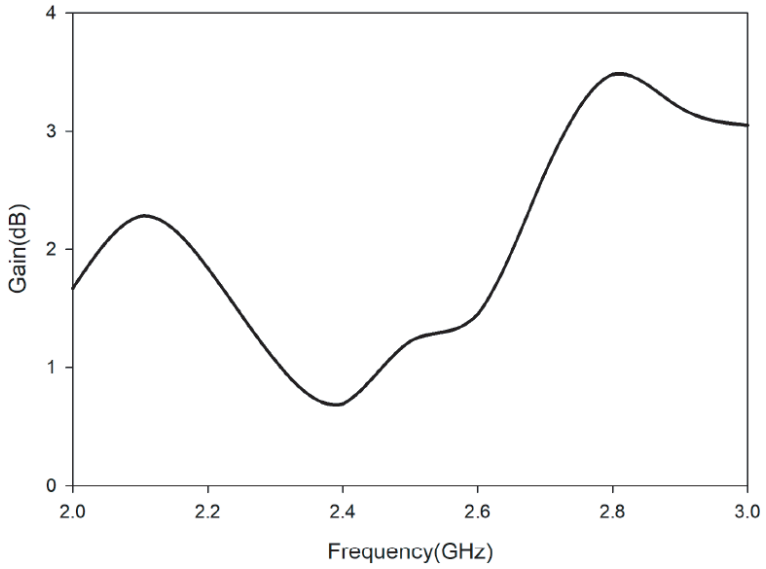

Figure 9. Measured gain of the reference antenna.

measured gain of the reference antenna is illustrated in Fig. 9. At the resonance frequency, a gain of 2.02 dB is observed. The simulated gain of the antenna as a function of frequency is also analyzed in the 2–3 GHz region. Initially, there is a decrease in gain with frequency. From 2.3 GHz onwards, there is an increase in gain with frequency. For the reference antenna an efficiency of 92.13% is obtained.

4.2. Antenna Loaded with Superstrate

A photograph of reference antenna loaded with superstrate is shown in Fig. 10.

When the antenna is loaded with superstrate, the periodic pattern with substrate provides a parasitic loading which results in improved matching. The bandwidth is not much affected by the presence of the superstrate. From the measured results, an impedance bandwidth of 374 MHz from 2.453 GHz to 2.827 GHz is observed for the antenna loaded with superstrate. In Fig. 11, a comparison of reflection characteristics of the reference antenna and the antenna loaded with superstrate is done. The variation in reflection characteristics with the variation in spacing between antenna and superstrate is shown in Fig. 12. It can be seen that neither the resonance frequency nor the magnitude of S_{11} is not much affected by the spacing variation.

It is well known that the gain of printed antennas can be improved by the use of a superstrate with proper parameters [2]. The gain can be further increased by printing periodic pattern on the

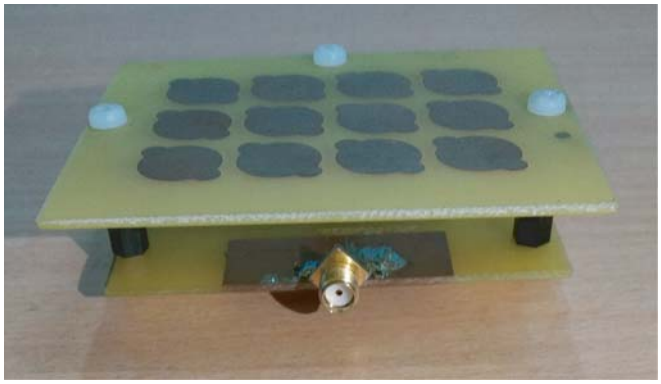

Figure 10. Antenna with superstrate.

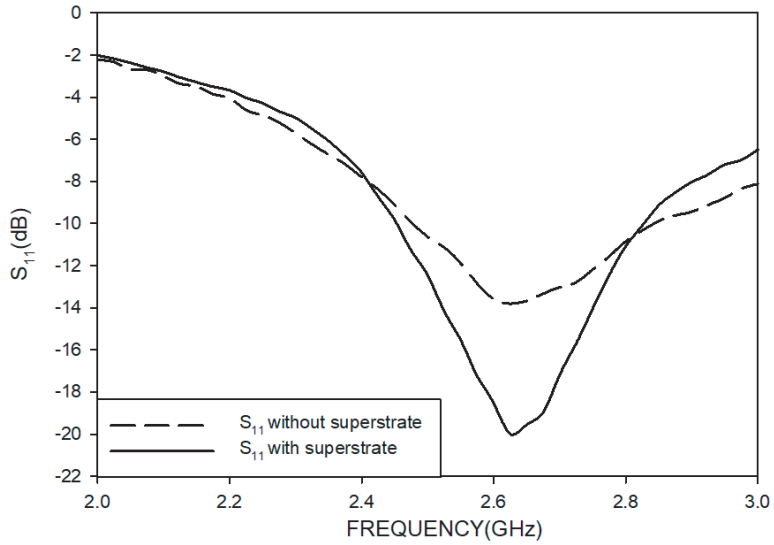

Figure 11. Reflection characteristics of reference antenna with and without superstrate.

superstrate. The simulation results show that the gain of the reference antenna is 1.96 dB at resonance frequency. The gain increases to 2.4 dB when a plain superstrate is used. When periodic pattern is printed on the superstrate, the gain further increases to 4.13 dB.

The measured gain of the reference antenna and the gain after adding the artificial dielectric superstrate are shown in Fig. 13. For the reference antenna at 2.65 GHz, a gain of 2.02 dB is observed. When the superstrate is added, the gain improves to 4.46 dB. At this frequency a high value of 18 is obtained for the effective permittivity of the artificial dielectric. Due to this high value of ϵ_r electric field confinement occurs which results in higher gain.

The gain is also a function of spacing between the antenna and the superstrate. The simulated results of variation in gain with respect to spacing is shown in Table 1. The optimum value of gain is obtained when the spacing is 20 mm.

The measured two-dimensional radiation patterns of the antenna with and without superstrate in XZ and YZ planes at 2.65 GHz for the co-polarization case are shown in Fig. 14. In the YZ plane the pattern is nearly omnidirectional, and a figure of 8 pattern is observed in the XZ plane. Comparing the radiation patterns with and without superstrate, the enhancement in gain can be clearly seen from the figure.

It can be seen that radiation patterns are more directive when the superstrate is added, as the superstrate directs the electromagnetic waves from the antenna towards boresight.

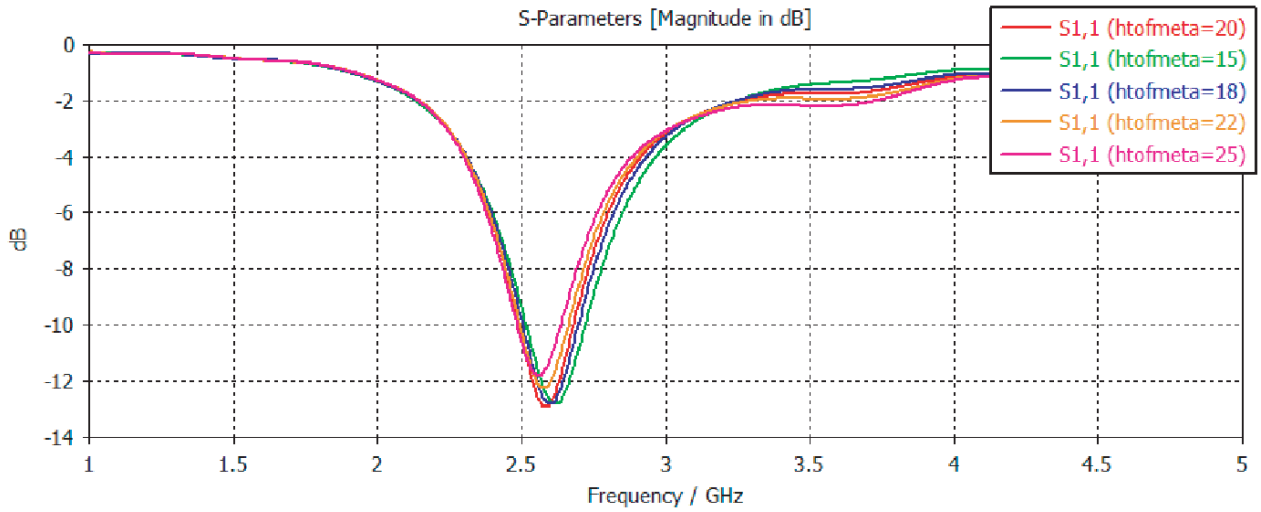

Figure 12. Variation of S_{11} with spacing between antenna and superstrate (htofmeta — spacing between antenna and superstrate).

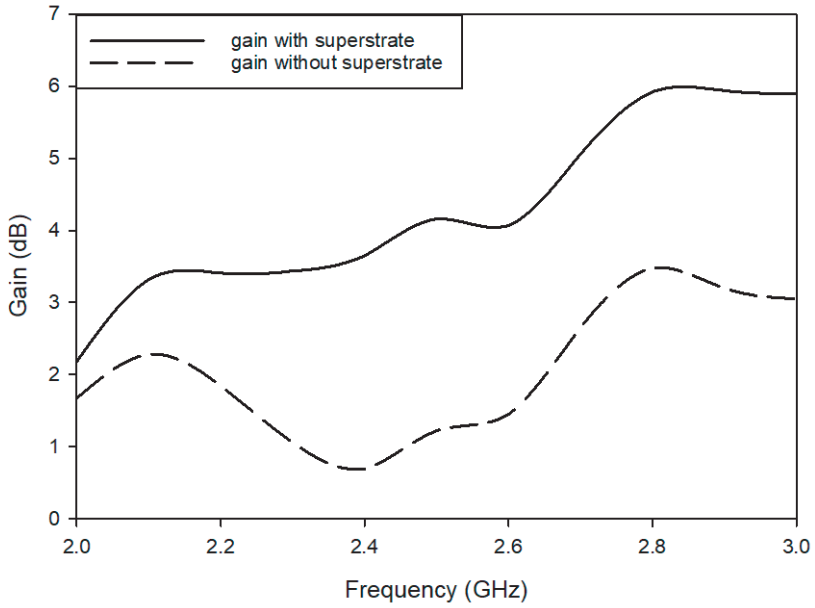

Figure 13. Measured gain of the reference antenna with and without superstrate.

Table 1. Variation of gain with spacing between antenna and superstrate.

Spacing between antenna and superstrate (mm)	gain (dB)
15	3.94
18	4.08
20	4.13
22	4.07
25	4.00

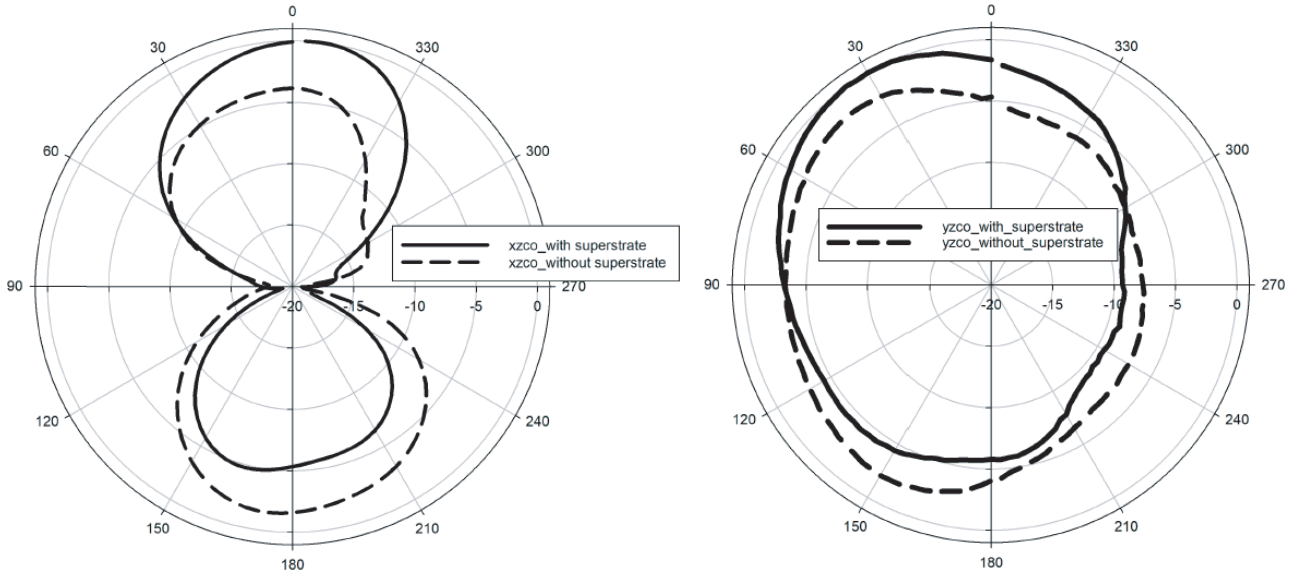

Figure 14. Measured two-dimensional co-polarization radiation pattern with and without superstrate for (a) XZ plane and (b) YZ plane.

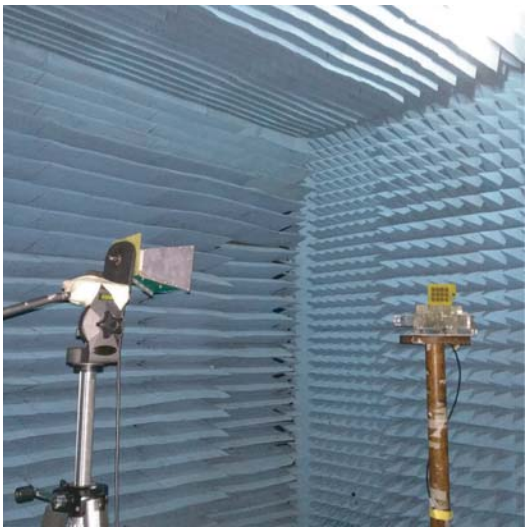

Figure 15. Radiation pattern measurement setup.

A photograph of the experimental setup for radiation pattern measurement is shown in Fig. 15.

5. CONCLUSION

In this paper, we have propose a technique for improving gain and impedance matching for a CPW-fed planar antenna. An artificial dielectric layer with a high value of effective permittivity is used as a superstrate. This artificial dielectric layer is formed by printing a finite size array of 3×4 unit cells on an FR-4 substrate. Compared with reference antenna, a gain enhancement of 2.50 dB is obtained when superstrate is used. The distance between the antenna and the superstrate is only $\lambda_0/6$ where λ_0 is the free space wavelength. Furthermore, the artificial superstrate helps in tilting the main beam towards boresight.

REFERENCES

1. Alexopoulos, N. and D. Jackson, "Fundamental superstrate (cover) effects on printed circuit antennas," *IEEE Transactions on Antennas and Propagation*, Vol. 32, No. 8, 807–816, 1984.
2. Jackson, D. and N. Alexopoulos, "Gain enhancement methods for printed circuit antennas," *IEEE Transactions on Antennas and Propagation*, Vol. 33, No. 9, 976–987, 1985.
3. Mittra, R., Y. Li, and K. Yoo, "A comparative study of directivity enhancement of microstrip patch antennas with using three different superstrates," *Microwave and Optical Technology Letters*, Vol. 52, No. 2, 327–330, 2010.
4. Ge, Y., K. P. Esselle, and Y. Hao, "Design of low-profile high-gain EBG resonator antennas using a genetic algorithm," *IEEE Antennas and Wireless Propagation Letters*, Vol. 6, 480–483, 2007.
5. Lee, Y. J., J. Yeo, R. Mittra, and W. S. Park, "Application of Electromagnetic Bandgap (EBG) superstrates with controllable defects for a class of patch antennas as spatial angular filters," *IEEE Transactions on Antennas and Propagation*, Vol. 53, No. 1, 224–235, 2005.
6. Chaimool, S., K. L. Chung, and P. Akkaraekthalin, "Simultaneous gain and bandwidths enhancement of a single-feed circularly polarized microstrip patch antenna using a metamaterial reflective surface," *Progress In Electromagnatics research B*, Vol. 22, 23–37, 2010.
7. Shaw, T., D. Bhattacharjee, and D. Mitra, "Gain enhancement of slot antenna using zero-index metamaterial superstrate," *International Journal of RF and Microwave Computer-Aided Engineering*, Vol. 27, e21078, 2016.
8. Kim, J. H., C. Ahn, and J. Bang, "Antenna gain enhancement using a holey superstrate," *IEEE Transactions on Antennas and Propagation*, Vol. 64, No. 3, 1164–1167, 2016.
9. Attia, H., L. Yousefi, M. M. Bait-Suwailam, M. S. Boybay, and O. M. Ramahi, "Enhanced-gain microstrip antenna using engineered magnetic superstrates," *IEEE Antennas and Wireless Propagation Letters*, Vol. 8, 1198–1201, 2009.
10. Syed, W. H. and A. Neto, "Front-to-Back ratio enhancement of planar printed antennas by means of artificial dielectric layers," *IEEE Transactions on Antennas and Propagation*, Vol. 61, No. 11, 5408–5416, 2013.
11. Sarkhel, A. and S. R. Bhadra Chaudhuri, "Enhanced-gain printed slot antenna using an electric metasurface superstrate," *Applied Physics A*, Vol. 122, No. 10, 934, 2016.
12. Attia, H., O. Siddiqui, and O. Ramahi, "Beam tilting of single microstrip antenna using high permittivity superstrate," *Microwave and Optical Technology Letters*, Vol. 55, No. 7, 1657–1661, 2013.
13. Pirhadi, A., H. Bahrami, and J. Nasri, "Wideband high directive aperture coupled microstrip antenna design by using a FSS superstrate layer," *IEEE Transactions on Antennas and Propagation*, Vol. 60, No. 4, 2101–2106, 2012.
14. Chen, X., T. M. Grzegorczyk, B.-I. Wu, J. Pacheco, Jr. and J. A. Kong, "Robust method to retrieve the constitutive effective parameters of metamaterials," *Phys. Rev. E*, Vol. 70, No. 1, 016608, 2004.
15. Buell, K., H. Mosallaei, and K. Sarabandi, "A substrate for small patch antennas providing tunable miniaturization factors," *IEEE Transactions on Microwave Theory and Techniques*, Vol. 54, No. 1, 135–146, 2006.
16. Mukherjee, B., P. Patel, and J. Mukherjee, "A novel hemispherical dielectric resonator antenna with complementary split-ring-shaped slots and resonator for wideband and low cross-polar applications," *IEEE Antennas and Propagation Magazine*, Vol. 57, No. 1, 120–128, Feb. 2015.
17. Sinha, M., V. Killamsetty, and B. Mukherjee, "Near field analysis of RDRA loaded with split ring resonators superstrate," *Microwave and Optical Technology Letters*, Vol. 60, No. 2, 472–478, 2018.
18. Simons, R. N., *Coplanar Waveguide Cicuits, Components and Systems*, John Wiley and Sons, New York, 2001.